

DRAFT APPENDIX

20 April, 2001

Data and analyses supporting the document “Independent populations of chinook salmon in Puget Sound”

The Puget Sound TRT: K. Currens, Northwest Indian Fisheries Commission; J. Doyle, U. S. Forest Service; R. Fuerstenberg, King Co. DNR; W. Graeber, Washington DNR; K. Rawson, Tulalip Tribes; M. Ruckelshaus and N. Sands, NMFS –Northwest Fisheries Science Center; and J. Scott, Washington Dept. of Fish and Wildlife.

Additional contributors to this report: E. Buhle, L. Holsinger, and T. Beechie, NMFS-NWFSC; A. Marshall and C. Busack, WDFW.

Note: An electronic copy of this Appendix and the accompanying main document are available in PDF format on the NMFS-NWFSC web site at
(<http://www.nwfsc.noaa.gov/cbd/trt/>).

Table of Contents

Appendix A.....	5
Methods and Results for less informative population indicators.	5
Direct observations of migration.....	6
Patterns in life history characters.....	7
Spatial synchrony in spawner abundance.....	8
Environmental effects on population synchrony.....	11
Habitat characteristics.....	13
Identifying Hydrologic Regions in Puget Sound.....	13
Comparisons of stream temperature among Puget Sound chinook spawning areas.....	15
EPA ecoregions.....	16
Geology.....	16
Appendix B: Data Tables.....	28

List of Tables

Table A.1. Straying matrix for Puget Sound chinook.....	17
Table B.1. Estimates of theta and Nm.....	29
Table B.2. Estimated time since divergence between sites.....	30
Table B.3. Cavalli-Sforza and Edwards' chord distance.....	31
Table B.4. Nei's (1978) genetic distance.....	32
Table B.5. P-values from pairwise G-tests for heterogeneity in allele frequencies at 29 loci.....	33
Table B.6. Absolute differences in mean yearly spawning dates.....	34
Table B.7. Dissimilarity matrix for smolt-spawner age distributions.....	36
Table B.8. Absolute differences in mean spawner length.....	37
Table B.9. Correlation coefficients for population abundance.....	38
Table B.10. Correlation matrix for stream gages in Puget Sound.....	39
Table B.11. Absolute difference in mean temperature during incubation....	40

List of Figures

Figure A.1. Dispersal curve for Puget Sound chinook.....	18
Figure A.2. Representative age distributions for Puget Sound chinook.....	19
Figure A.3. Length-at-age of Puget Sound chinook.....	20
Figure A.4. Relationships among Puget Sound chinook in abundance.....	21
Figure A.5. Spatial correlogram for spawner abundance.....	22
Figure A.6. Classification tree for hydroregions.....	23
Figure A.7. Runoff-pattern regions in Puget Sound.....	24
Figure A.8. Clustering of Puget Sound spawning areas based on temperature...	25
Figure A.9. EPA's Level IV Ecoregions.....	26
Figure A.10. Geology of Puget Sound.....	27

Appendix A

Methods and Results for less informative population indicators

The following section describes data analyses and results for population indicators that were not as influential in delineating population boundaries as those reported in the main population identification document (“Independent populations of chinook salmon in Puget Sound”; available electronically at <http://www.nwfsc.noaa.gov/cbd/trt/>). The indicators reported in this section are those believed to be informative for identifying independent populations in a theoretical sense; but because of data quality issues, confounding sources of variation, or uncertainty in interpretation of results, the TRT did not rely heavily on these results in making their determinations. We include the analyses and results here for completeness. Furthermore, we hope to encourage further data collection, experimentation or discussion of the natural levels of variation in these indicators and how they might suggest something about population structure of chinook salmon in Puget Sound.

Direct observations of migration

Methods

Some direct observations of straying among Puget Sound chinook stocks were available. Most of these observations were based on releases and subsequent recoveries of hatchery chinook marked with coded-wire tags, available in a database maintained by the Pacific States Marine Fisheries Commission (RMPC 1997). We searched the database for all records of tagged chinook that were reared in watersheds in Puget Sound or the Strait of Juan de Fuca and recovered at or near the probable location of spawning (i.e., hatchery rack, spawning ground, carcass survey, and freshwater trap recoveries). These data allowed us to estimate rates of straying; straying is defined as recovery of a tagged fish at a location other than its rearing site. Stray rate refers to the proportion of all fish in a tag group (or from a release site) that are recovered somewhere other than their tagging/release site. However, stray rate estimates must be viewed with caution because methods of estimating the total number of returning tagged fish vary among recovery locations and the geographic area sampled for strays is not comprehensive or selected based on a spatially stratified design. Estimates of straying rates based on small-scale experimental studies were available in a few locations.

We graphically examined the relationship between straying rate and dispersal distance in all coded-wire tagged release groups that produced at least 20 freshwater recoveries ($n = 3 - 98$ groups per release site). Sixteen release sites distributed throughout Puget Sound were selected and summarized. Here, straying rates were measured separately for each release group as the proportion of recoveries that occurred at a given nautical distance from the release location.

Results

The pattern of releases and recoveries of tagged chinook (Table A.1) suggests that rates of migration between basins or major subbasins in Puget Sound are generally quite low. For most stocks, $> 95\%$ of the tag recoveries from spawners occurred within the same subbasin where the juveniles were released (but see the caveat above regarding estimates of stray rates based on these data). However, some migration between major basins does occur. For example, spring/summer-run chinook released at Kendall Creek Hatchery on the North Fork Nooksack have been recovered in the North Fork Stillaguamish, and summer-run fish from the North Fork Stillaguamish have returned to the Snoqualmie basin. A small number of adults have been recovered outside of Puget Sound; e.g., spring-run chinook of Suiattle River origin released from Marblemount Hatchery have returned to the Cowlitz Hatchery on the lower Columbia River.

The dispersal curve for all locations and release groups (Fig. A.1) shows a strongly nonlinear decline in straying rate as a function of distance between release and recovery locations, with the steepest decline occurring between zero and approximately 75 km. We did not attempt to model this relationship statistically. The individual dispersal curves from 16 individual release sites (results not shown) suggest that the shapes of dispersal distributions are highly variable among streams and stocks. For example, the number of fish recovered at greater than 100 km from the source was very low for a

number of release groups (e.g., those from Grovers, Skookum, and Garrison creeks, and Wallace River). In contrast, fish recoveries at greater than 100 km from the source occurred from tag groups originating in the Elwha River, North Fork Stillaguamish, Marblemount hatchery, Skokomish River, and Kendall Creek.

Patterns in life history characters

Methods

Data on spawner age (A. Marshall and C. Busack, WDFW, pers. comm.) and age at outmigration (WDFW 1995) were obtained by reading scales collected from carcasses on the spawning grounds. Scale samples for spawner age were taken from the same wild and hatchery stocks used in the genetic analyses, and sample sizes varied among stocks ($n \geq 40$). Patterns in age structure were examined by calculating an index of percentage overlap in age distributions (both spawner age and spawner/outmigrant age) for all pairwise combinations of stocks. The resulting similarity matrices were then used in UPGMA cluster analysis.

Similar to the age-structure data, length (fork length or post-orbital length or both) was measured from all chinook adults collected for genetic analyses on the spawning grounds (A. Marshall and C. Busack, WDFW, unpublished data). Fish were grouped by age (3, 4, and 5 year olds) and sex for initial length analyses. If multiple brood years within an age and sex class existed, they were combined to increase the number of stocks with adequate sample size for analyses. Only 3 year old males and 4 year old males and females had large enough sample sizes for length-at-age cluster analyses ($n \geq 40$). In most cases, length data were reported as either fork length or post-orbital length, so regressions were performed within each age and sex class to standardize lengths to post-orbital length (regression R^2 ranged from 0.80 to 0.93). Differences in length between 4 year old males and females were not statistically significant (ANOVA $df = 1$, $P > 0.12$), so the sexes were pooled for cluster analyses of 4 year olds. Differences in the mean length-at-age between all sites sampled were computed and used to generate a difference matrix for 4 year old males and females combined. The matrix was then used in a UPGMA cluster analysis to generate a dendrogram.

Results

Representative age distributions of Puget Sound chinook spawners based on carcass samples are shown in Fig. A.2. A log-linear model including only naturally produced stocks detected highly significant overall heterogeneity in spawner age distributions ($G^2 = 674.83$, $df = 63$, $P < 0.0001$). In general, the cluster analysis based on overlap in spawner age distributions (result not shown) does not indicate any strong patterns of similarity concordant with the spatial distribution of stocks, although there are some exceptions (e.g., the Cedar River and Issaquah Hatchery stocks cluster together, as do the upper Cascade River spring-run, lower Sauk River summer-run, and Cascade Hatchery stocks). Distributions of age at outmigration and spawning also are shown in Fig. A.2.

An overall test for heterogeneity was not performed on distributions of age at outmigration and spawning. The UPGMA dendrogram developed from the combined data on age at outmigration and spawning (not shown) shows 2 main clusters, one containing all spring-run stocks and a few summer/fall stocks (i.e., Wallace, Sauk, Snoqualmie and Elwha). The other main cluster in the dendrogram is a collection of summer/fall stocks from throughout Puget Sound, with no geographic pattern to the degree of similarity in juvenile/spawner age distributions.

Age-specific length varies significantly among 26 stocks of Puget Sound Chinook (ANOVA $F = 8.24$, $df = 25$, $P < 0.001$; Fig. A.3). The UPGMA dendrogram (not shown) indicates that unlike the age data, patterns in length-at-age of Puget Sound chinook are fairly concordant with the spatial arrangement of streams. Fish in streams that are closer together have more similar length-at-age than fish from streams that are farther apart.

Spatial synchrony in spawner abundance

Methods

We obtained time series of spawner abundance for Puget Sound chinook from StreamNet (NMFS, unpublished database). Time series with < 10 yr of data were excluded from the analysis, as were abundance data for hatchery-produced stocks, although natural spawners in some areas include a substantial proportion of first-generation hatchery strays. Using these criteria, we selected 31 stocks (loosely defined here to mean any group of fish for which relevant data were available) to use in the analysis. Most of these correspond to SASSI stocks (WDF et al. 1993), but several groups of spawners in small, independent Puget Sound tributaries not described by WDF et al. (1993) were also included. The time series for each stock consists of annual total spawning escapement, as estimated from counts of live spawners, carcasses, or redds in selected index stream reaches. The series range in length from 10 to 30 yr, and most include 1997 as the most recent sample year. In order to meet the requirements of statistical time series models, missing observations that were not at the beginning or end of the series were interpolated by averaging the abundance in the years immediately preceding and following the missing point. Only four values were interpolated, so the error introduced by this procedure was minimal.

The abundance data were filtered using standard time series methods prior to the correlation analyses. Because our goal was to examine covariation in abundance that might be due to the exchange of migrants between stocks, we first attempted to eliminate sources of variation within stocks that were not likely attributable to immigration or emigration (cf. Hanski and Woiwod 1993, Bjørnstad et al. 1999). Statistically, these sources of variation include (1) long-term temporal trends (which might be caused by changing environmental conditions due to natural or human causes) and (2) temporal autocorrelation (due to density-independent variation in cohort strength or autocorrelation in climate or other environmental variables). We assumed that these relatively long-term

patterns are driven by deterministic processes over long time scales because migration rates in salmonid populations are more likely to vary over short time scales (see references in McElhany et al. 2000). We recognize that even after accounting for trends and autocorrelation, we cannot assume that all sources of spurious correlation in abundance time series have been completely removed. Therefore, inferences about possible migration rates between groups based on these abundance time series should be made with caution.

Temporal trend was estimated separately for each time series using a third-order polynomial multiplicative model (Thomas 1996):

$$N_t = N_0 \ddot{e}_1^t \ddot{e}_2^{t^2} \ddot{e}_3^{t^3} e^{\hat{a}_t}, \quad (1)$$

where N_t is abundance in year t , the \ddot{e}_i are the trend parameters, and \hat{a}_t is a normal random variable. Eq. 1 is equivalent to

$$\log N_t = \hat{a}_0 + \hat{a}_1 t + \hat{a}_2 t^2 + \hat{a}_3 t^3 + \hat{a}_t, \quad (2)$$

where $\hat{a}_0 = \log N_0$ and $\hat{a}_i = \log \ddot{e}_i$ for $i > 0$. A third-order polynomial model was chosen because it was sufficiently complex to describe most of the obvious long-term patterns in the abundance data. The parameters in Eq. 2 (hereafter the ‘trend model’) were estimated by least squares, and a stepwise procedure was then used to find the most parsimonious model, based on Mallows’ C_p -statistic (Weisberg 1985:216, MathSoft 1998:157). Thus the final trend model for any particular stock did not necessarily include all three polynomial terms, but only those that contributed to the overall explanatory power of the regression.

Residuals from each polynomial trend regression were inspected visually to check the assumption that \hat{a}_t are normally distributed. Residuals for many stocks showed significant temporal autocorrelation, so a time series model with both trend and autoregressive parameters (Edwards and Coull 1987) was fitted to each abundance time series. This model (hereafter the ‘trend-AR model’) is:

$$\log N_t = \hat{a}_0 + \hat{a}_1 t + \hat{a}_2 t^2 + \hat{a}_3 t^3 + \hat{a}_1 \log N_{t-1} + \hat{a}_2 \log N_{t-2} + \Lambda + \hat{a}_p \log N_{t-p} + \hat{a}_t, \quad (3)$$

where N_{t-i} is the abundance in year $t-i$, the \hat{a}_i are autoregressive parameters, and the other variables and parameters are defined as in Eq. 2. The order p of the autoregression for each stock was chosen by fitting various autoregressive models (with $p \leq 8$) to the residuals from the trend model and selecting the most parsimonious model based on the Akaike Information Criterion (Burnham and Anderson 1998, MathSoft 1998:692). Once the order of the autoregression was determined, the parameters in the trend-AR model were estimated simultaneously by least squares.

The residuals from the trend and trend-AR time series models formed two new datasets which served as the input for the correlation analyses. Each set of residuals was used to compute a matrix of product-moment correlation coefficients between all pairs of stocks. The length of the residual time series varied among stocks, so correlations

between residuals from the trend model were computed in two ways: using pairwise deletion of missing observations (so that elements in the correlation matrix were based on differing sample sizes) and using casewise deletion (so that all correlation coefficients were based on $n = 10$ observations corresponding to years 1987-1996). Casewise deletion of missing observations could not be used in the correlation matrix based on trend-AR residuals because the dataset had too few years with data on all stocks.

Patterns of cross-correlation between stocks were examined by UPGMA cluster analysis with $1-r$ as the pairwise distance measure. The robustness of the resulting clusters was assessed by jackknifing over years. Each of the 30 years in the escapement dataset was successively deleted and the correlation matrix was recalculated on the reduced dataset. Each correlation matrix was used in a UPGMA cluster analysis, and a consensus tree based on the 30 dendrograms was found using program CONSENSE in the PHYLIP computer package (Felsenstein 1993). This procedure allows an evaluation of the sensitivity of the correlation matrix to inclusion of extreme observations in particular years. The jackknifing analysis was performed only on the dataset consisting of residuals from the trend-AR model.

Spatial autocorrelation in abundance was investigated by testing the association between pairwise correlation coefficients and pairwise geographic distances separating the spawning grounds of stocks, as described above (*Genetic structure of Puget Sound chinook: Methods*). In addition, the relationship between distance and correlation in abundance was statistically modeled in order to estimate the spatial scale of demographic synchrony. We used a Gaussian model (Myers et al. 1997, Bradford 1999),

$$\rho(d) = \rho_0 \exp\left(-\frac{d^2}{2\sigma^2}\right),$$

in which the demographic correlation $\rho(d)$ between two stocks declines monotonically with increasing distance d , starting at an initial value of ρ_0 when $d = 0$. This model can accommodate a ‘threshold’ distance $d = \sigma$ at which the correlation decays most rapidly. The model was fit using nonlinear least squares. No attempt was made to account for the nonindependence of elements in the correlation and distance matrices.

Results

For a majority of stocks, residuals from the trend model show significant serial autocorrelation, indicating that the trend-AR model is the more appropriate model for these stocks. Interestingly, there is no general pattern of strong autocorrelation at a lag of 3-5 yr, as would be expected to result from density-independent variation in cohort strength, given the predominant age at reproduction of Puget Sound chinook.

The jackknifed consensus tree for the cluster analysis based on trend-AR residuals (not shown) indicates that low-level structure in the correlation matrix (i.e., clusters of 2-4 stocks) is generally robust to the deletion of single years from the dataset. Higher-level structure, however, is much more sensitive to the inclusion or exclusion of particular years. The relationships among stocks indicated by the dendrogram are summarized graphically on a map of Puget Sound by color-coded symbols representing the spawning

grounds of each stock (Fig. A.4). Clusters of stocks depicted in Fig. A.4 are those clusters that are joined at a linkage distance ≤ 0.55 in the dendrogram. This linkage distance corresponds roughly to a statistically significant correlation coefficient for a sample size of $n = 9$, which is the smallest sample size used in the correlation matrix.

On the whole, the relationships among stocks suggested by correlations in abundance are not concordant with the pattern suggested by geography and genetic similarity, i.e., geographically proximate stocks do not consistently show stronger correlations in abundance than geographically distant stocks. This conclusion is supported by inspection of the spatial correlogram based on trend-AR residuals (Fig. A.5). Although a one-tailed Mantel test indicated a significant ($P < 0.05$) negative association between the correlation coefficient and geographic distance, the relationship is weak. Fig. A.5 shows the fit of the Gaussian decay model. The estimate of the “threshold” parameter is $\sigma = 86.6$, indicating that positive correlations tend to occur at a distance of ≤ 86.6 km. This value is significantly different from zero (approximate t -test, $P < 0.001$). However, the initial correlation is quite low ($\rho_0 = 0.15$), although it too is significantly different from zero ($P < 0.01$).

One of the most striking examples of a group of neighboring stocks with highly correlated dynamics is the group consisting of the lower Skagit River fall-run, upper Skagit River summer-run, and lower Sauk River summer-run stocks. This cluster is robust to different methods of computing the correlation matrix and filtering the abundance time series (results not shown). On the other hand, these Skagit basin stocks also cluster with the geographically distant Dungeness River and Area 7A stocks (Fig. A.4). The upper Sauk River and Suiattle River spring-run stocks, which spawn in the upper reaches of the Skagit basin, appear unrelated to the lower Skagit basin stocks in all the cluster analyses. The summer- and fall-run stocks in the Stillaguamish River cluster together, but only when the correlation matrix is based on trend-AR residuals (Fig. A.4; results of simple trend models not shown). In contrast, the summer-run stocks in the Stillaguamish and Snohomish Rivers appear related when the correlation matrix is based on residuals from the trend model (results not shown). In the analysis based on trend-AR residuals, the Duwamish/Green River, Cedar River, and north Lake Washington stocks form a cluster, as do the Wallace River and Snohomish River summer-run stocks.

Environmental effects on population synchrony

Methods

In order to investigate the possibility that the observed cross-correlations in abundance were due to correlated environmental influences (i.e., the Moran effect) rather than demographic exchange (e.g., Harrison and Quinn 1989, Lande et al. 1999, Ripa 2000, Bjørnstad et al. 1999, Kendall et al. 2000), we examined the relationships between annual spawner abundance and some environmental variables. The rationale for this approach was that if the environmental variables explain a significant amount of the variance in abundance, then their effects could be removed from the abundance time

series and the between-stock correlations recalculated. We chose to focus on two hydrologic variables, peak discharge during the incubation period and low flow during the upriver spawning migration, because previous studies indicated that these variables have strong effects on salmonid vital rates that may be detectable in spawner escapement data (Beamer and Pess, unpublished manuscript). Time series of discharge measured at stream gages on or near the spawning grounds of Puget Sound chinook stocks were obtained from the United States Geological Survey. Gage data were available for 22 of the 31 stocks. Peak flow during incubation was defined as the maximum instantaneous discharge observed between 1 September and 31 March of each brood year. Low flow during spawning migration was defined as the minimum 7-d mean flow observed between 1 May and 31 October of each return year. Scatterplots of abundance (both the raw number of spawners and the residuals from the time series models) against peak and low flow were used to check visually for effects of the hydrologic variables. Because peak discharge is hypothesized to affect egg-to-fry survival and most chinook in Puget Sound spawn between the ages of 3 and 5, we used lagged scatterplots with the peak flow time series lagged by 3, 4, or 5 yr. Low flows during summer and early fall may delay migrating spawners, increase stress-related mortality, or prevent access to spawning grounds, so abundance in each year was plotted against low flow observed in the same year.

Results

Lagged scatterplots do not suggest a systematic relationship between spawner abundance and instantaneous peak flow at a time lag of 3, 4, or 5 yr in any stock (results not shown). This conclusion is not altered when residuals from the time series models, rather than raw or log-transformed escapement estimates, are used as the index of abundance. Similarly, scatterplots of spawner abundance against 7-d summer low flow provide no evidence of any relationship between these variables (results not shown). It is clear from inspection of the scatterplots that attempting to statistically model the relationship between peak flow and abundance would not be informative for the question we are addressing. In summary, in interpreting correlations in time series of abundance data, we cannot distinguish between correlations due to correlated environmental conditions experienced by groups of fish and those due to migrants between two groups. For this reason, we feel that the level of inference from population synchrony analyses is relatively low.

Habitat characteristics

Identifying Hydrologic Regions in Puget Sound

Methods

We performed a set of analyses intended to classify all the rivers and streams in Puget Sound into hydrologic regions on the basis of hydrologic patterns and the physical variables mean basin elevation and mean annual precipitation. An understanding of regional hydrologic regimes can provide insights into the selective environment fish experience, and therefore illuminate a potential influence on population structure. These analyses are especially useful in areas where genetic, abundance and life history data are not informative. For example, winter hydrologic conditions, such as low flow and cold temperatures in high elevations, influence the intra-gravel environment and the success of overwintering of eggs and alevins (Blachut 1988), which could in turn affect spawn timing.

We used a two-step process to identify hydrologic regions. First, we identified distinct groups of streams based on the overall hydrograph pattern observed at a sample of stream gages. Secondly, we used a classification tree analysis to identify broad hydrologic regions across Puget Sound to describe hydrographs in areas where gage data were not available. These two steps are described in detail below.

(1) Identifying streamflow patterns based on annual hydrograph—Time series of monthly mean discharge (cfs) at 52 United States Geological Survey (USGS) stream gages located throughout Puget Sound were obtained from the Washington Department of Ecology. The time series included 8-74 years of data, depending on the gage. The USGS gages included in this analysis had at least a 10-year period of record, little to no artificial regulation, and were located within or adjacent to chinook spawning habitat.

For each gage, the log-transformed monthly means were averaged over all years, producing an “average” annual hydrograph. The average hydrographs were treated as variables with 12 observations (one observation per month) and rank correlation coefficients between these variables were computed for all pairs of gages. Using correlation coefficients to measure similarity between gages emphasizes the timing and relative magnitude of peak and low flows, ignoring differences in the total magnitude of flow. The correlation matrix was used in a UPGMA cluster analysis with $1-r_s$ as the distance measure.

(2) Identifying hydrologic regions using predictive models. Because gage data were not available for all stream reaches where chinook are known to spawn, we developed empirical models to predict hydrograph pattern using known, easily measured variables. We chose average basin elevation, defined as the average elevation of all points upslope of a given point, and average annual precipitation as predictors for several reasons. One, previous studies in Puget Sound (e.g. Beechie 1992, Amerman and Orsborn 1987) found predictive relationships between these variables and a variety of hydrologic characteristics. Secondly, measurements of elevation and precipitation were easily obtained for the entire region. Because the models were fitted using data on gage

characteristics reported by USGS, rather than GIS data layers, three gages were omitted from the analysis because elevation and precipitation measurements were not available.

Models were developed using a parametric version of classification tree analysis (Venables and Ripley 1994). Classification tree analysis predicts group membership on the basis of known variables enabling us to predict hydrograph patterns for all of Puget Sound based on hydrograph patterns at a set of streamflow gages. These classification tree models use a recursive partitioning algorithm to construct a binary decision tree, similar to a taxonomic key, in which observations are classified into pre-defined categories (in this case, the four hydrograph types, R, RS, SR and S, identified in the above streamflow pattern analysis) based on their scores on one or more predictor variables (elevation and precipitation). Data for mean basin elevation and mean annual precipitation were obtained for each USGS gage from Williams et al. 1985.

In the classification tree analysis, the observations in each node of the tree are partitioned into two daughter nodes by choosing the split along the range of a single predictor that maximizes the log-likelihood over all possible splits of all predictors, where the likelihood is based on a multinomial model for the frequencies of the categories (Venables and Ripley 1994). The splitting continues until a stopping criterion is reached (in this case, nodes were not split when they contained two or fewer observations). The tree can then be “pruned” back by sequentially eliminating terminal nodes and computing Akaike’s Information Criterion (AIC) for each of the nested sub-trees (Burnham and Anderson 1998, Venables and Ripley 1994). The sub-tree with the lowest AIC score is selected as the most parsimonious model for the data. Because the sample size was small relative to the number of estimated parameters in the fully fitted tree, the small-sample correction AIC_c was used in addition to AIC (Burnham and Anderson 1998), and the results of pruning on the two criteria were compared.

Based on the breakpoints identified above, we mapped the resulting hydrologic regions using Geographic Information Systems (GIS) analysis. We used 30-meter Digital Elevation Model (DEM) data from USGS to calculate mean basin elevation across Puget Sound. We combined the mean basin elevation data with mean annual precipitation data for 1961-1990 (Daly and Taylor 1998) to produce a hydroregion map.

Results

(1) Identifying streamflow patterns based on annual hydrograph. Hydrographs of mean monthly flow showed three basic patterns: (1) a rainfall-dominated pattern (hereafter R) with a winter peak and low flows in August-September (e.g., Issaquah Creek), (2) a snowmelt-dominated pattern (S) with a peak in May-July and low flows in late winter or early spring (e.g., Suitttle River), and (3) an intermediate pattern with both rainfall- and snowmelt-driven peaks and low flows typically in August-September (Fig. A.6). The intermediate category was further subdivided into streams (e.g., Duckabush River) whose highest peaks are driven by rainfall (RS) and those (e.g., White River) whose highest peaks are due to snowmelt (SR). This classification was supported by the UPGMA dendrogram (not shown), which showed four main clusters of streams based on hydrograph pattern.

(2) *Identifying hydrologic regions using predictive models.* The classification tree analysis resulted in a AIC-selected classification tree with six terminal nodes (the terminal nodes represent the predictive classification scheme defined by the tree, with predicted values equal to the most common category in the node). This tree had an overall misclassification rate of 6/49. That is, the predicted hydrograph category was incorrect for 6 of the 49 gages in the sample – whereas the tree with the lowest value of AIC_c had only two terminal nodes and an overall misclassification rate of 13/49. Because the AIC-selected tree seemed clearly over-fitted but the two-node AIC_c -selected tree was not predictively useful, we chose a tree of intermediate complexity to use for prediction. This tree had five terminal nodes and an overall misclassification rate of 7/49 (Fig. 14). For this tree, $AIC = 0.5$ and $AIC_c = 8.65$, where $AIC_i = AIC_i - \min\{AIC_j \text{ for all candidate models } j\}$. Thus it was not the most parsimonious model, but represented a reasonable compromise between the two criteria.

In the final tree, the discriminations among hydrograph types were based primarily on average basin elevation (Fig. A.6). Streams with average elevation < 2595 ft generally had type R hydrographs. Between 2595 and 3110 ft, most streams were type RS. Streams between 3110 and 4285 ft were generally type SR, as were streams above 4285 ft that experience < 101.5 in of precipitation annually. Only streams above 4285 ft with > 101.5 in of precipitation were predicted to be type S. Figure A.7 shows the resulting 4 hydroregions mapped across Puget Sound, together with the SASSI chinook populations.

Comparisons of stream temperature among Puget Sound chinook spawning areas

Methods

Time series of monthly temperature at 47 river and stream monitoring stations were obtained from the Washington Department of Ecology. The data consisted of temperatures taken once to several times a month, for only portions of the year or all months of the year. Two analyses were conducted on stream temperature. The first analysis examined the pattern of stream temperatures throughout all months of the year (contingent on data availability). For this analysis, we calculated monthly mean temperatures for each station across all years, producing an “average” annual stream temperature profile. Then, similar to the stream hydrograph pattern analysis, mean annual temperature profiles were treated as variables and rank correlation coefficients were calculated for pairwise combinations of variables. The resulting correlation matrix was used in UPGMA cluster analysis.

The second analysis evaluated differences between the average stream temperatures during the incubation period of the various chinook populations. Here, we restricted data to temperatures during the 3-month period following the median spawning date for each index area where chinook are surveyed. Note, chinook spawning surveys were not conducted in the vicinity of 11 of the 47 temperature monitoring stations. In these cases, the median spawn date for the nearest index area was used for choosing the beginning of the 3-month incubation period. Stream temperatures were averaged over the 3-month incubation period for each station and across all years, producing an “average” monthly

stream temperature. Differences between average monthly stream temperatures were calculated for pairwise combinations of all stations resulting in a matrix for UPGMA cluster analysis.

Results

For the first analysis examining annual stream temperature profiles, all stations demonstrated a similar pattern where temperatures are cool in the winter, rise to a peak in summer, and decline again during fall. The primary differences in the temperature profiles were apparent in the slopes of incline and decline, and the range of temperatures. These differences, however, were not well resolved through UPGMA cluster analysis. The UPGMA dendrogram (not shown) did not show any distinct groupings of streams based on similarity in temperature profiles. Similarly, differences in stream temperature during the chinook incubation period were not found with UPGMA cluster analysis. The resulting dendrogram (Fig. A.8) did not show any notable groupings between temperature stations.

EPA ecoregions

The U.S. Environmental Protection Agency (EPA) has defined ecoregions based on a number of characteristics—geology, physiography, soils, land use patterns, vegetation, climate, wildlife, and hydrology. The ecoregions are defined based on scales over which the above characteristics are relatively homogeneous. These ecoregions may partly describe differences in the selective environments chinook experience throughout Puget Sound. EPA defines ecoregions on a number of different spatial scales—we have summarized 2 of those scales (or levels) for evaluating habitat characteristics and their possible relation to population structure. The EPA has divided the North American continent into 78 regions at Level III (not shown). Four main Level III Ecoregions occur within Puget Sound, including: North Cascades, Puget Lowland, Cascades and the Coast Range. The EPA has also developed finer scale, Level IV ecoregions for portions of the United States, including Puget Sound (Fig. A.9). At Level IV, 15 main ecoregions occur within Puget Sound.

Geology

The U.S. Geologic Survey (USGS) developed geologic maps for various western states using 40 different classifications. Distinct geological characteristics may partly describe differences in the selective environments chinook experience throughout Puget Sound. The Interior Columbia Basin Ecosystem Management Project digitized and combined these state maps into one map (<http://www.icbemp.gov>). We simplified the 40 geologic classifications into 10 main categories as follows: alluvium, calc-alkaline igneous, carbonate, glacial drift, gneiss, mafic igneous, meta-sandstone, phyllite and schist, sedimentary and ultramafic (Fig. A.10).

TABLE A1. Straying matrix for Puget Sound chinook. Except where indicated, data are based on recoveries of coded-wire tagged chinook reared at hatcheries within Puget Sound, as reported by PSMFC. In general, hatchery stocks were included in the matrix only if the original broodstock was of local wild origin or if the present-day stock is genetically similar to the local wild population; however, some stocks with substantial out-of-basin influence are included to increase geographic coverage. These stocks are indicated by italics. Only recoveries that indicate the location where an individual likely would have spawned (hatchery rack, spawning ground, freshwater fish trap, or carcass survey recoveries) are reported. Shaded cells indicate recoveries of tagged chinook within the same basin or subbasin where they were reared (i.e., successful homing). Note that recoveries are grouped geographically and may include both hatchery returns and wild spawners within a given basin. Counts of recovered tags should be interpreted cautiously for three reasons. First, straying rates of hatchery chinook likely differ from straying rates of wild fish, particularly where the hatchery stock has been substantially influenced by out-of-basin introductions. Second, most counts shown in the table are summed over multiple tagged release groups and brood years, and the number and date of releases differ among stocks. Third, counts from different locations or years may not be directly comparable because of differences in methods used to estimate the total number of returns based on the number of tags sampled and sampling efficiency. In particular, some recoveries do not provide an estimate of sampling efficiency and simply report the number of tags observed. Thus the counts should not be directly interpreted as estimates of straying rates.

Stock or Rearing Location																	
	Nooksack Basin		Skagit Basin			Stillaguam. Basin	Snohomish Basin		Lk. Wash. Basin	Green Basin	Puyal. Basin	Nisqually Basin	South Puget Sound	Kitsap Peninsula	Skokomish Basin	Dungeness Basin	Elwha Basin
Recovery Basin	Kendall Sp	Skookum Sp	Marblemount Sp	Marblemount Su I	Wild Skagit Su	NF Stilla Su	Wallace Su	Wallace F	Issaquah F	Soos Cr F	White Sp	Nisqually F	Garrison (Chambers Cr) F	Grovers Cr F	Skokomish F	Dungeness	Elwha F
Nooksack	58	6								2.03							
NF Nooksack	4966.11	10.19															
MF Nooksack	7																
SF Nooksack	6.35	238.26															
Samish	1						1			2.08							
Skagit	5.37			20	7	20.4											
Lower Skagit	1					6											
Upper Skagit	7.02		1465.7	115.03	3.13	4		2.03						1			
Cascade	6.74		77.26														
Stillaguamish						5											
NF Stillaguamish	15.01		1			1050.97											
SF Stillaguamish				3													
Snohomish							5.69	9						1.02			
Skykomish							16.12/1099*										
Wallace			2.03	1		10.06	752.48/8913*	369.1		3							
Bridal Veil/NF Sky							636*										
Snoqualmie						30.87	119*			3.25							
Issaquah									1094.07					3.07			

Table A1 Continued

	Nooksack Basin		Skagit Basin			Stillaguam. Basin	Snohomish Basin		Lk. Wash. Basin	Green Basin	Puyal. Basin	Nisqually Basin	South Puget Sound	Kitsap Peninsula	Skokomish Basin	Dungeness Basin	Elwha Basin
Recovery Basin	Kendall Sp	Skookum Sp	Marblemount Sp	Marblemount Su I	Wild Skagit Su	NF Stilla Su	Wallace Su	Wallace F	Issaquah F	Soos Cr F	White Sp	Nisqually F	Garrison (Chambers Cr) F	Groves Cr F	Skokomish F	Dungeness	Elwha F
Lk Washington										1			1				
Green									9.77	5766.87				8.9			
Puyallup										1.34	6.03						
White										1	3530.89			1	1.03		
Garrison Hatch.	1.04								3	2.01			74.6	18.32			
Nisqually												1347.3					
McAllister Hatch.												1	1	8.6			
Capitol Lake									20.1					6.44	2.24		1
Burley Cr														5.41			
Coulter Cr														1	7.74		
Minter Hatch.									1					11.02	1		

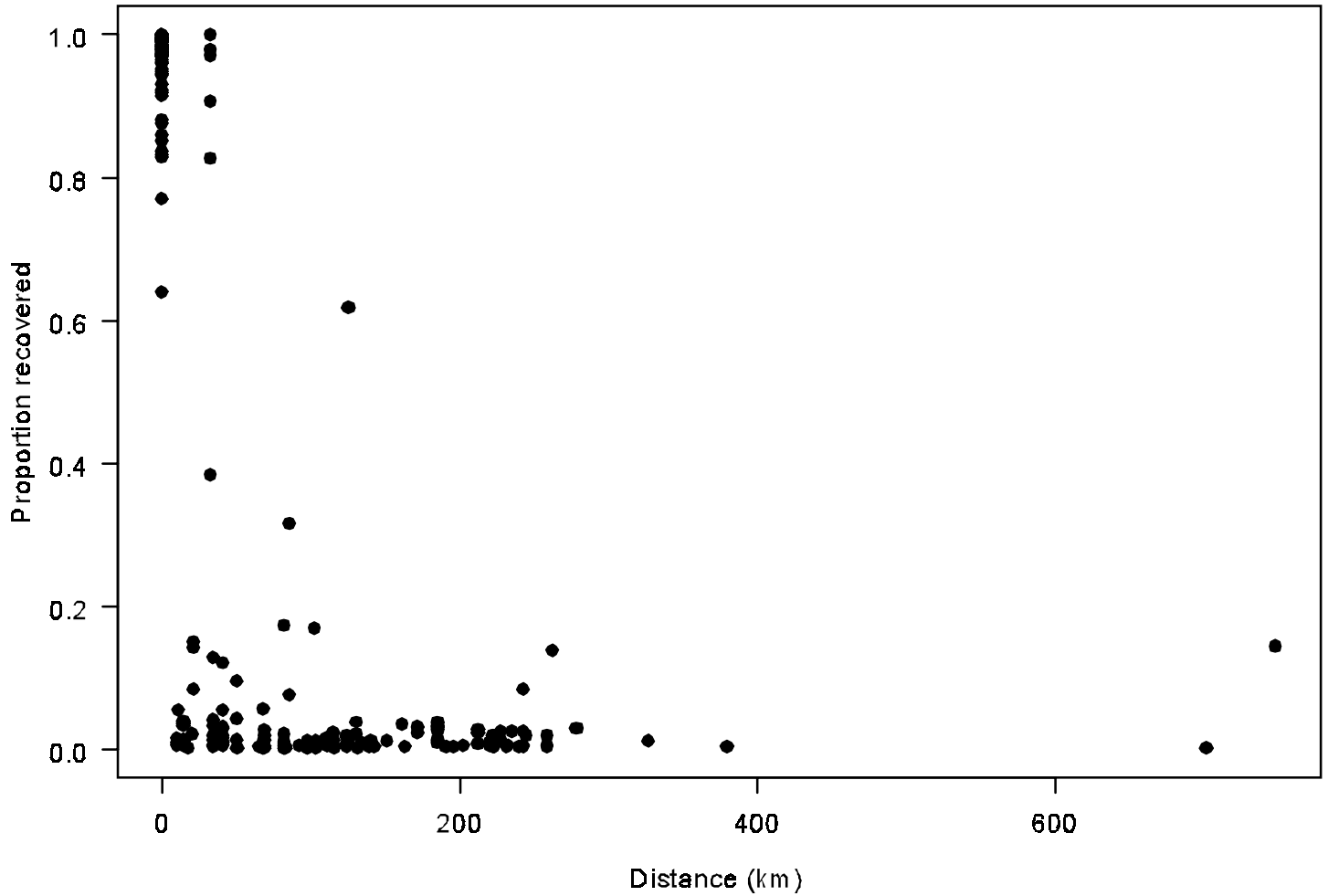


FIGURE A1. Dispersal curve for Puget Sound chinook based on coded-wire tag recoveries. Data shown here represent a total of 167 tagged release groups from 15 hatcheries for which at least 20 tagged spawners were recovered. Each point is the proportion of recoveries that occurred at a given distance from the release location. Proportions are calculated separately for each release group, so multiple dispersal "curves" are overlaid in the figure.

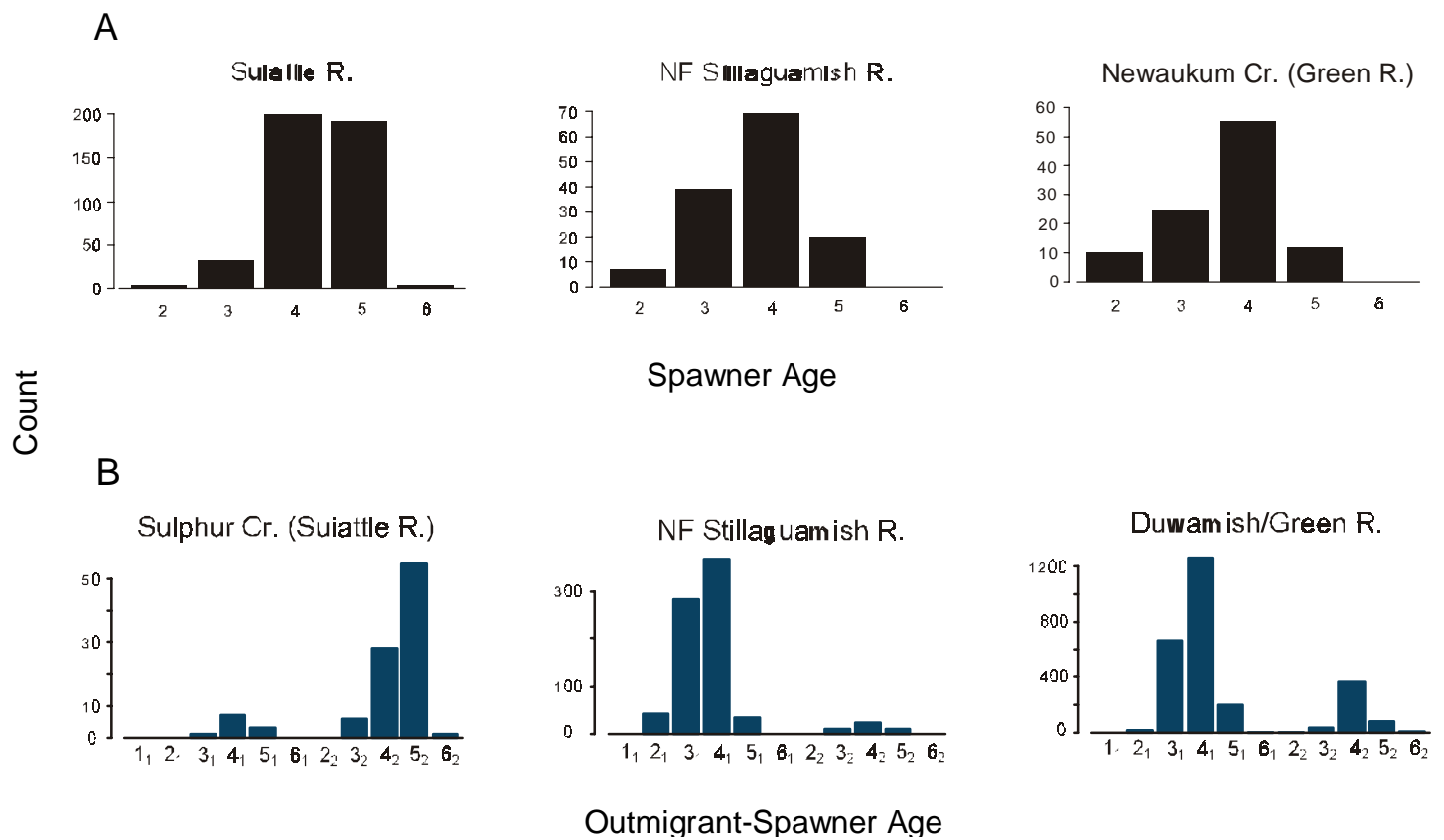


FIGURE A2. Representative age distributions for Puget Sound chinook stocks, based on scale samples from carcasses on spawning grounds. (A) Distributions of spawner age. (B) Distributions of age at outmigration (the subscripted number) and spawning (the large number). All ages are expressed as year of life, beginning with egg deposition.

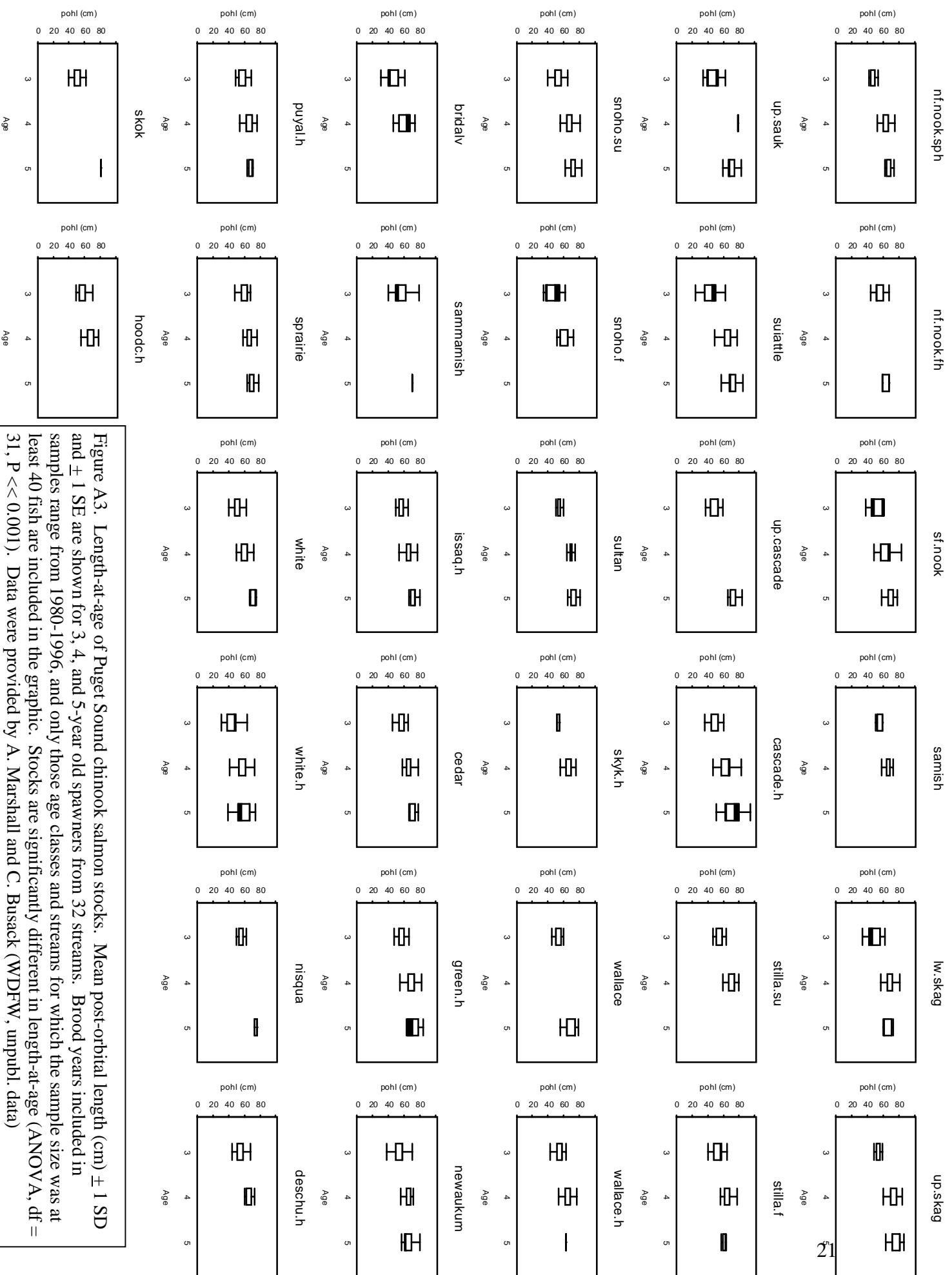


Figure A3. Length-at-age of Puget Sound chinook salmon stocks. Mean post-orbital length (cm) ± 1 SD and ± 1 SE are shown for 3, 4, and 5-year old spawners from 32 streams. Brood years included in samples range from 1980-1996, and only those age classes and streams for which the sample size was at least 40 fish are included in the graphic. Stocks are significantly different in length-at-age (ANOVA, $df = 31$, $P < 0.001$). Data were provided by A. Marshall and C. Busack (WDFW, unpubl. data)

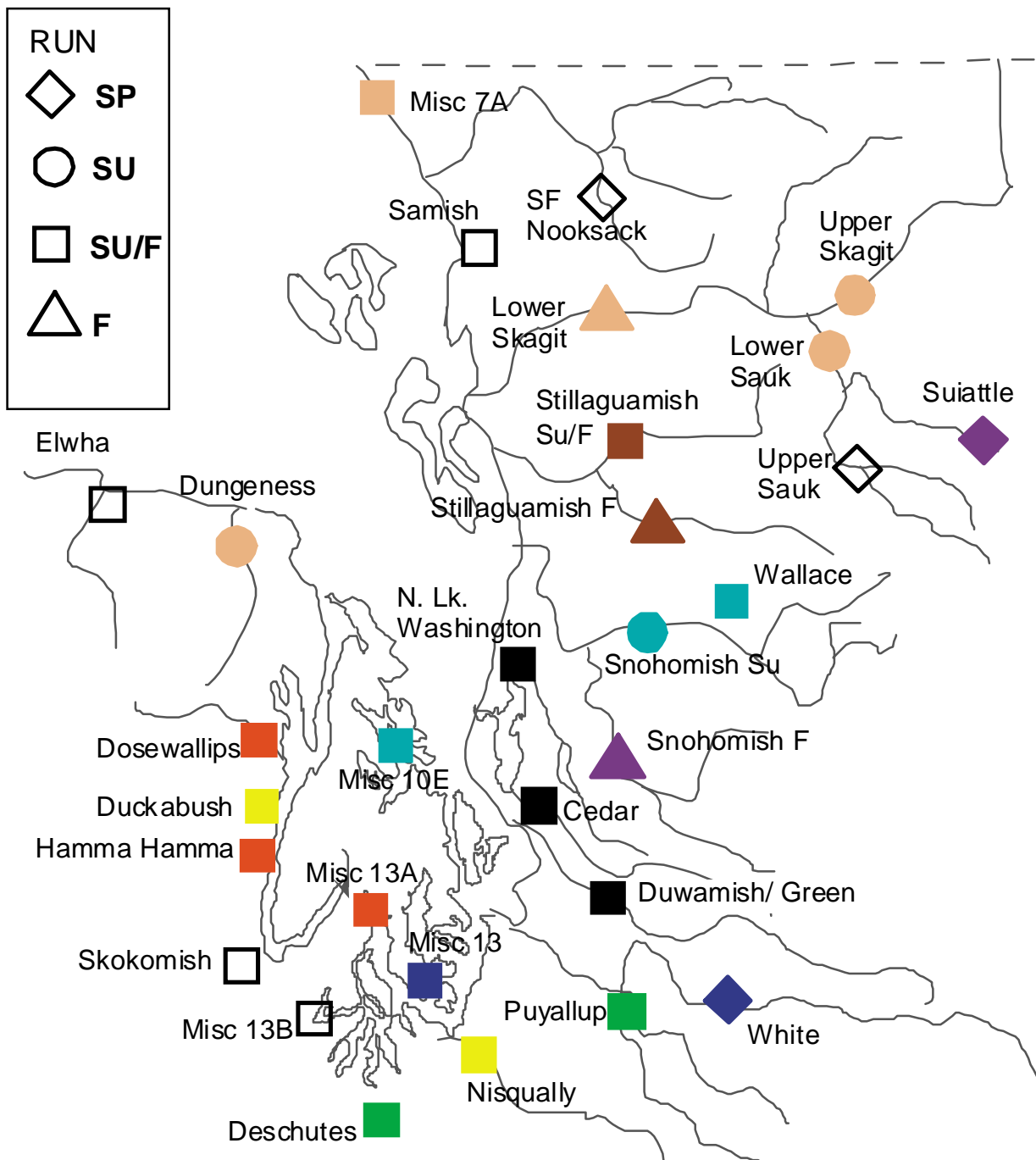


FIGURE A4. Relationships among Puget Sound chinook stocks, based on UPGMA cluster analysis using temporal correlation in abundance as the similarity measure. The correlation matrix was calculated from trend-AR model residuals, using pairwise missing data deletion. Clusters were defined by taking all groups in the dendrogram that were joined at linkage distance ≥ 0.55 . The clusters defined in this way are represented on the map by distinct colors, with hollow symbols indicating "independent" stocks that are in clusters by themselves. Shapes of symbols indicate run-timing categories.

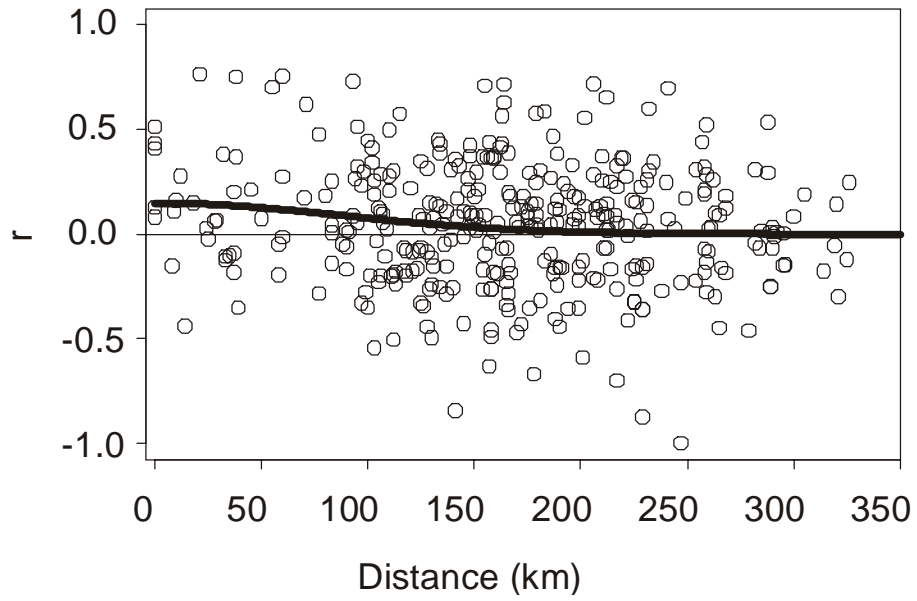


FIGURE A5. Spatial correlogram for spawner abundance in Puget Sound chinook stocks. The correlation in abundance between each pair of stocks (based on trend-AR model residuals) is plotted against the geographic distance separating the spawning areas of those stocks. The solid line is the Gaussian decay model fit to the correlation and distance data (see *Methods: Temporal correlations in spawner abundance*).

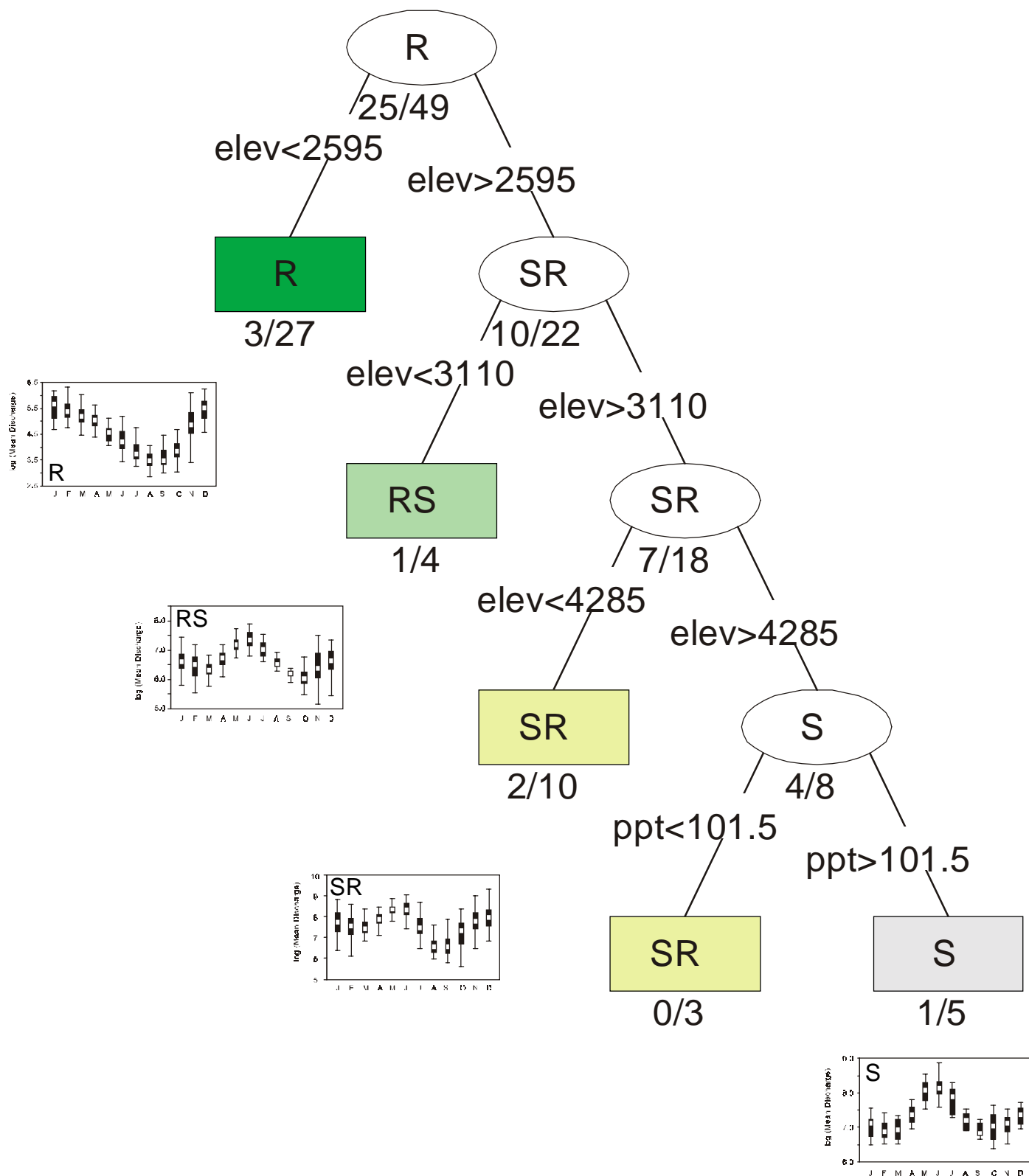


FIGURE A6. Classification tree used to predict hydrograph type from average basin elevation (ft) and average annual precipitation (in). The hydrograph categories (R = rainfall-dominated, RS = rainfall-/snowmelt-dominated, SR = snowmelt-/rainfall-dominated, S = snowmelt-dominated) correspond to the clusters identified by UPGMA cluster analysis; typical examples of each category are shown. The category indicated on each terminal node (the colored squares) is the predicted hydrograph type for the observations in that node. The fraction of observations in each node that are incorrectly classified is indicated under the node. Details of the algorithm used to generate the tree are given in the text.

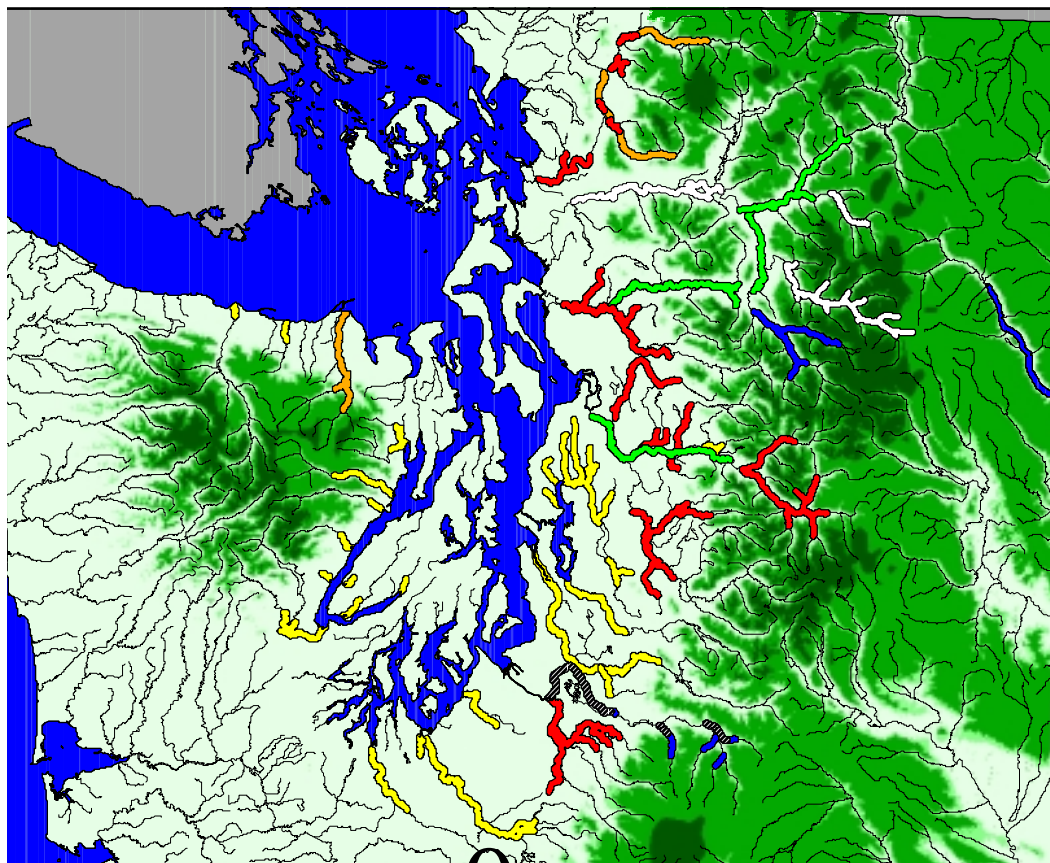


Figure A7. Runoff-pattern regions in Puget Sound derived from mean basin elevation and mean annual precipitation using classification tree analysis. Four main runoff patterns were detected including: Rainfall dominated, Rainfall transition, Snowmelt transition and Snowmelt dominated.

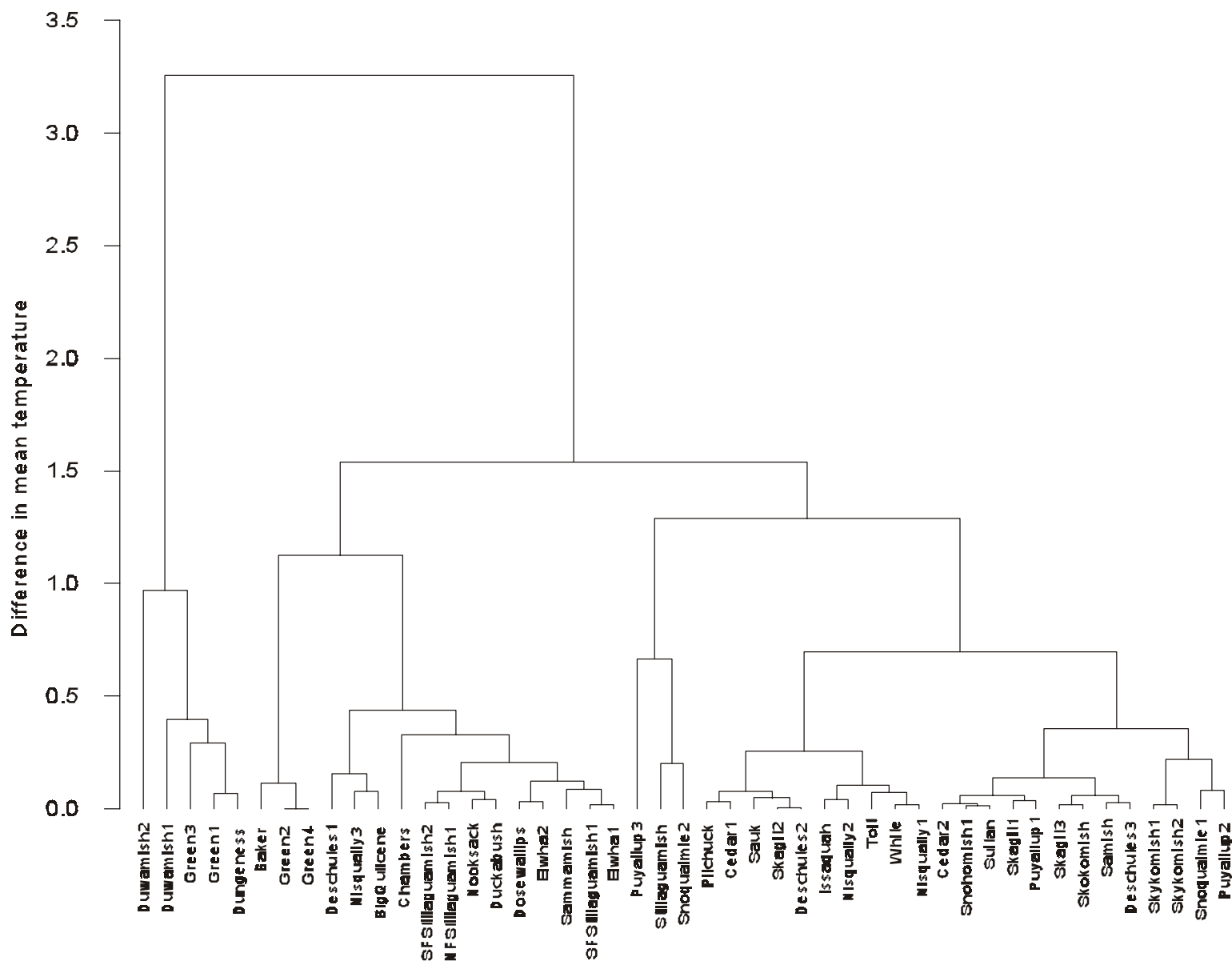


FIGURE A8. Clustering of Puget Sound chinook spawning areas based on differences in mean temperature during chinook egg incubation. Mean incubation temperature in each area is based on an assumed 3-month incubation period beginning on the median date of chinook spawning in the nearest index survey area. Absolute difference in mean temperature was the dissimilarity measure used in the UPGMA cluster analysis.

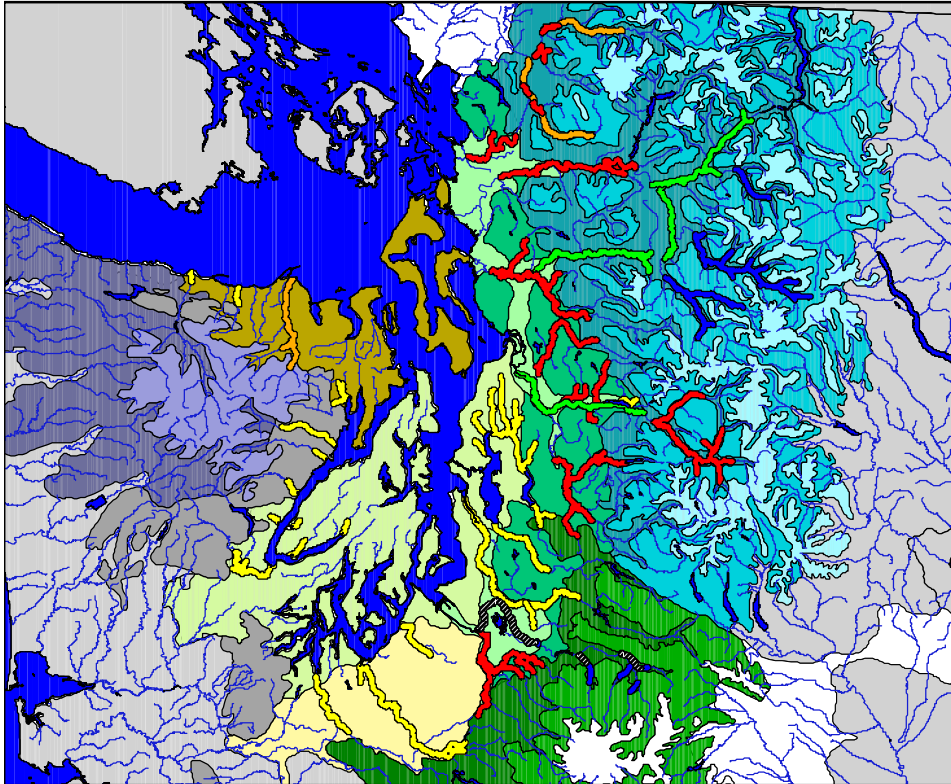


Figure A9. The Environmental Protection Agency's Level IV Ecoregions in Puget Sound. Ecoregions represent areas of general similarity in an ecosystem, and in quality and quantity of environmental resources.

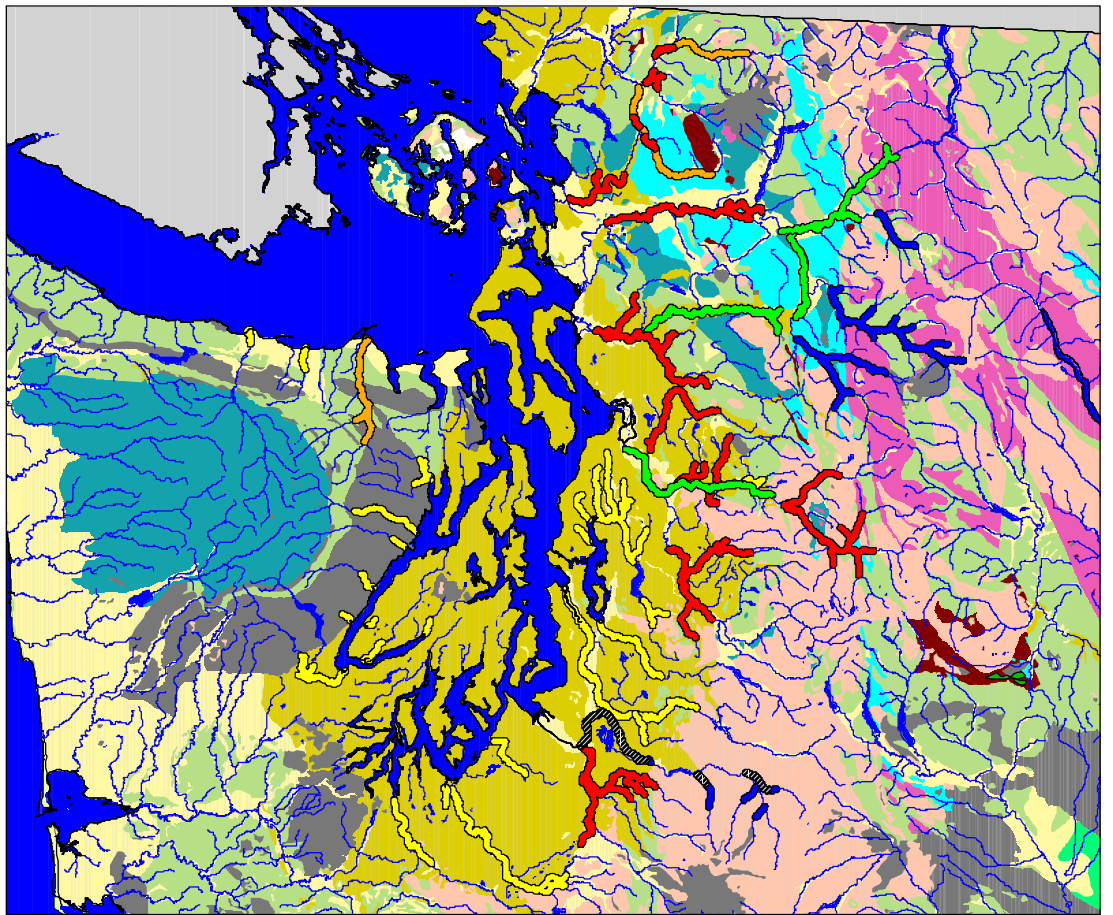


Figure A10. Geology of Puget Sound region using 10 major lithology types derived from U.S.G.S. data (www.icbemp.gov).

Appendix B

Data Tables

The following section includes results from data analyses conducted as part of the TRT's efforts to identify demographically independent populations of chinook salmon in Puget Sound. Not all data were explicitly considered by the TRT for each indicator—they are included here for completeness and to spur collection of additional data. The data are summarized in a matrix format for each watershed. Values in each cell represent some measure of distance or difference between the two sites being considered. Methods for calculating differences between sites for each data type are described in the text of the main document or in this Appendix.

Table B.1. Estimates of theta (above diagonal) and Nm (below diagonal).

NOOKSACK	sf.nook	nf.nook
sf.nook	**	0.024
nf.nook	10.321	**

SKAGIT	lw.skag	up.skag	lw.sauk	up.sauk	suiattle	cascade
lw.skag	**	0.016	0.157	0.013	0.025	0.089
up.skag	15.605	**	0.111	0.015	0.046	0.110
lw.sauk	1.342	2.011	**	0.091	0.237	0.376
up.sauk	19.076	15.942	2.499	**	0.057	0.145
suiattle	9.899	5.207	0.807	4.157	**	0.028
cascade	2.558	2.031	0.416	1.477	8.635	**

STILLAGUAMISH	nf.stilla	sf.stilla
nf.stilla	**	0.051
sf.stilla	4.679	**

SNOHOMISH	lw.snoh	skykom	sultan	wallace	bridalveil	snoqual
lw.snoh	**					
skykom		**	0.012	0.003	0.000	0.007
sultan		19.999	**	0.008	0.010	0.013
wallace		82.641	30.216	**	0.000	0.005
bridalveil		-753.262	23.712	-521.083	**	0.006
snoqual		35.317	19.582	52.084	40.707	**

LK. WASHINGTON	cedar	nlk.wash	sammam	issaquah
cedar	**		0.008	0.012
nlk.wash		**		
sammam	32.520		**	0.012
issaquah	21.328		20.488	**

SOUTH SOUND	duwam.gr	newauk	puyallup	white	nisqually	deschut
duwam.gr	**		0.004	0.024	0.005	0.001
newauk	-295.061	**	0.007	0.021	0.002	0.002
puyallup	59.688	36.151	**	0.019	0.016	0.008
white	10.009	11.559	12.663	**	0.019	0.026
nisqually	50.275	135.916	15.223	13.156	**	0.012
deschut	416.417	103.787	29.424	9.524	20.160	**

Table B.2. Estimated time since divergence between sites (t , in generations).

NOOKSACK	sf.nook	nf.nook
sf.nook	**	7.1
nf.nook		**

SKAGIT	lw.skag	up.skag	lw.sauk	up.sauk	suiattle	cascade
lw.skag	**	98.4	324.8	17.9	41.9	67.3
up.skag		**	274.3	24.7	94.4	90.1
lw.sauk			**	96.0	313.4	285.1
up.sauk				**	55.0	84.4
suiattle					**	16.6
cascade						**

STILLAGUAMISH	nf.stilla	sf.stilla
nf.stilla	**	25.7
sf.stilla		**

SNOHOMISH	lw.snoh	skykom	sultan	wallace	bridalveil	snoqual
lw.snoh	**					
skykom		**		5.1	-0.6	19.3
sultan			**			
wallace				**	-0.6	7.2
bridalveil					**	10.3
snoqual						**

LK. WASHINGTON	cedar	nlk.wash	sammam	issaquah
cedar	**			
nlk.wash		**		
sammam			**	
issaquah				**

SOUTH SOUND	duwam.gr	newauk	puyallup*	white	nisqually	deschut
duwam.gr	**		19.9		7.2	
newauk		**				
puyallup			**		20.4	
white				**		
nisqually					**	
deschut						**

Table B.3. Cavalli-Sforza and Edwards' chord distance

NOOKSACK	sf.nook	nf.nook
sf.nook	*****	
nf.nook	0.0748	*****

SKAGIT	lw.skag	up.skag	lw.sauk	up.sauk	suiattle	cascade
lw.skag	*****					
up.skag	0.0382	*****				
lw.sauk	0.0573	0.0514	*****			
up.sauk	0.0528	0.0385	0.056	*****		
suiattle	0.0523	0.0317	0.0543	0.0418	*****	
cascade	0.0575	0.0439	0.0669	0.0491	0.0439	*****

STILLAGUAMISH	nf.stilla	sf.stilla
nf.stilla	*****	
sf.stilla	0.0713	*****

SNOHOMISH	lw.snoh	skykom	sultan	wallace	bridalveil	snoqual
lw.snoh	*****					
skykom		*****				
sultan		0.0518	*****			
wallace		0.0418	0.0451	*****		
bridalveil		0.0433	0.0513	0.0437	*****	
snoqual		0.0486	0.0566	0.0536	0.0573	*****

LK. WASHINGTON	cedar	nlk.wash	sammam	issaquah
cedar	*****			
nlk.wash		*****		
sammam	0.0573		*****	
issaquah	0.0472		0.0478	*****

SOUTH SOUND	duwam.gr	newauk	puyallup*	white	nisqually	deschut
duwam.gr	*****					
newauk	0.0244	*****				
puyallup*	0.0394	0.0461	*****			
white	0.0511	0.0531	0.0614	*****		
nisqually	0.0533	0.0499	0.0627	0.0677	*****	
deschut	0.0356	0.0361	0.048	0.0595	0.0596	*****

HOOD CANAL	skokom	hamma*	ducka	dosewal
skokom	0			
hamma*	0.0488	0		
ducka			0	
dosewal				0

Table B.4. Nei's (1978) genetic distance.

NOOKSACK	sf.nook	nf.nook
sf.nook	*****	
nf.nook	0.003	*****

SKAGIT	lw.skag	up.skag	lw.sauk	up.sauk	suiattle	cascade
lw.skag	*****					
up.skag	0.0007	*****				
lw.sauk	0.0005	0.0002	*****			
up.sauk	0.0009	0.0007	0.0004	*****		
suiattle	0.0016	0.0006	0.0009	0.0007	*****	
cascade	0.0012	0.0004	0.0011	0.0008	0.0009	*****

STILLAGUAMISH	nf.stilla	sf.stilla
nf.stilla	*****	
sf.stilla	0.0043	*****

SNOHOMISH	lw.snoh	skykom	sultan	wallace	bridalveil	snoqual
lw.snoh	*****					
skykom		*****				
sultan		0.0018	*****			
wallace		0	0.001	*****		
bridalveil		0	0.0018	0	*****	
snoqual		0.0008	0.0024	0.0009	0.0015	*****

LK. WASHINGTON	cedar	nlk.wash	sammam	issaquah
cedar	*****			
nlk.wash		*****		
sammam	0.0013		*****	
issaquah	0.0007		0.0008	*****

SOUTH SOUND	duwam.gr	newauk	puyallup*	white	nisqually	deschut
duwam.gr	*****					
newauk	0	*****				
puyallup*	0.0005	0.0007	*****			
white	0.001	0.0008	0.0008	*****		
nisqually	0.0004	0	0.001	0.0015	*****	
deschut	0.0002	0.0004	0.0003	0.0014	0.0007	*****

Table B.5. P-values from pairwise G-tests for heterogeneity in allele frequencies at 29 loci.

NOOKSACK	sf.nook	nf.nook
sf.nook	*****	
nf.nook	0	*****

SKAGIT	lw.skag	up.skag	lw.sauk	up.sauk	suiattle	cascade
lw.skag	*****					
up.skag	0.0086	*****				
lw.sauk	0.0006	0.0042	*****			
up.sauk	0	0.0032	0.0009	*****		
suiattle	0	0	0	0	*****	
cascade	0	0.0043	0	0.0011	0.0002	*****

STILLAGUAMISH	nf.stilla	sf.stilla
nf.stilla	*****	
sf.stilla	0	*****

SNOHOMISH	lw.snoh	skykom	sultan	wallace	bridalveil	snoqual
lw.snoh	*****					
skykom		*****				
sultan		0.0001	*****			
wallace		0.2673	0.0273	*****		
bridalveil		0.2276	0.0011	0.3247	*****	
snoqual		0.0009	0	0.0002	0	*****

LK. WASHINGTON	cedar	nlk.wash	sammam	issaquah
cedar	*****			
nlk.wash		*****		
sammam	0		*****	
issaquah	0.0029		0.0384	*****

SOUTH SOUND	duwam.gr	newauk	puyallup*	white	nisqually	deschut
duwam.gr	*****					
newauk	0.6926	*****				
puyallup*	0.0111	0.0013	*****			
white	0	0	0	*****		
nisqually	0.0071	0.0263	0.0006	0	*****	
deschut	0.1283	0.1593	0.0073	0	0.0013	*****

HOOD CANAL	skokom	hamma*	ducka	dosewal
skokom	*****			
hamma*	0.1359	*****		
ducka			*****	
dosewal				*****

Table B.6. Absolute differences (d) in the overall mean of yearly weighted mean spawning dates. Bold entries indicate significant differences in two-sample t-tests using a basinwise Bonferroni-adjusted alpha level. Italics indicate that no test could be performed because fewer than 3 annual means were available.

NOOKSACK												
nooksack.r	0.0	9.2	11.1	17.2	4.4							
sf.nooksack.r	9.2	0.0	1.9	8.0	13.6							
mf.nooksack.r	11.1	1.9	0.0	6.1	15.5							
nf.nook_kendall.cr	17.2	8.0	6.1	0.0	21.6							
nf.nook_canyon.cr	4.4	13.6	15.5	21.6	0.0							
SKAGIT												
lw.skagit	0.0	17.9	16.0	27.2	61.4	65.0	56.3	55.7	53.3	15.6	24.9	21.7
up.skagit	17.9	0.0	1.9	9.3	43.6	47.1	38.4	37.9	35.4	2.3	7.1	3.8
lw.sauk	16.0	1.9	0.0	11.2	45.5	49.0	40.3	39.8	37.3	0.4	8.9	5.7
up.sauk	27.2	9.3	11.2	0.0	34.3	37.8	29.1	28.6	26.1	11.6	2.3	5.5
suiattle_big.cr	61.4	43.6	45.5	34.3	0.0	3.6	5.2	5.7	8.2	45.9	36.5	39.7
suiattle_tenas.cr	65.0	47.1	49.0	37.8	3.6	0.0	8.7	9.3	11.7	49.4	40.1	43.3
suiattle_buck.cr	56.3	38.4	40.3	29.1	5.2	8.7	0.0	0.5	3.0	40.7	31.4	34.6
suiattle_lime.cr	55.7	37.9	39.8	28.6	5.7	9.3	0.5	0.0	2.5	40.2	30.8	34.0
suiattle_sulphur.cr	53.3	35.4	37.3	26.1	8.2	11.7	3.0	2.5	0.0	37.7	28.3	31.6
up.skagit_illabot.cr	15.6	2.3	0.4	11.6	45.9	49.4	40.7	40.2	37.7	0.0	9.4	6.1
cascade.r	24.9	7.1	8.9	2.3	36.5	40.1	31.4	30.8	28.3	9.4	0.0	3.2
up.skagit_bacon.cr	21.7	3.8	5.7	5.5	39.7	43.3	34.6	34.0	31.6	6.1	3.2	0.0
STILLAGUAMISH												
nf.stillagua	0.0	5.3	20.9									
nf.stilla_squire.cr	5.3	0.0	15.6									
sf.stilla_jim.cr	20.9	15.6	0.0									
SNOHOMISH												
snohomish	0.0	9.3	11.8	2.7	3.0	2.7						
sultan.r	9.3	0.0	2.5	6.6	6.3	12.0						
wallace.r	11.8	2.5	0.0	9.1	8.8	14.5						
bridal_veil.cr	2.7	6.6	9.1	0.0	0.3	5.4						
snoqualmie.r	3.0	6.3	8.8	0.3	0.0	5.7						
snoqual_tolt.r	2.7	12.0	14.5	5.4	5.7	0.0						
LK. WASHINGTON												
n.lkwash_swamp.cr	0.0	13.6	19.5	18.3	19.8	21.7						
n.lkwash_north.cr	13.6	0.0	5.9	4.6	6.2	8.1						
n.lkwash_big_bear.cr	19.5	5.9	0.0	1.2	0.3	2.2						
n.lkwash_cottage.lake	18.3	4.6	1.2	0.0	1.5	3.5						
issaquah.cr_holder.cr	19.8	6.2	0.3	1.5	0.0	1.9						
cedar.r	21.7	8.1	2.2	3.5	1.9	0.0						
SOUTH SOUND												
duwamish_green.r	0.0	8.3	2.4	3.7	3.3	4.4	10.1	14.2	1.1	5.2	1.4	6.5
green_crisp.cr	8.3	0.0	5.8	12.0	4.9	3.9	1.9	6.0	7.1	3.0	9.6	14.7
green_newaukem.cr	2.4	5.8	0.0	6.2	0.9	2.0	7.7	11.8	1.3	2.8	3.8	8.9
puyal_clarks.cr	3.7	12.0	6.2	0.0	7.1	8.1	13.8	18.0	4.9	8.9	2.3	2.7
white_r_stuck.r	3.3	4.9	0.9	7.1	0.0	1.1	6.8	10.9	2.2	1.9	4.7	9.8
white_boise.cr	4.4	3.9	2.0	8.1	1.1	0.0	5.7	9.8	3.3	0.8	5.8	10.9
white_clearwater.r	10.1	1.9	7.7	13.8	6.8	5.7	0.0	4.1	9.0	4.9	11.5	16.6
white_greenwater.r	14.2	6.0	11.8	18.0	10.9	9.8	4.1	0.0	13.1	9.0	15.6	20.7
puyal_carbon.r	1.1	7.1	1.3	4.9	2.2	3.3	9.0	13.1	0.0	4.1	2.5	7.6
puyal_south_prairie.cr	5.2	3.0	2.8	8.9	1.9	0.8	4.9	9.0	4.1	0.0	6.6	11.7
nisqua_kapowsin.cr	1.4	9.6	3.8	2.3	4.7	5.8	11.5	15.6	2.5	6.6	0.0	5.1
nisqually.r	6.5	14.7	8.9	2.7	9.8	10.9	16.6	20.7	7.6	11.7	5.1	0.0
nisqua_ohop.cr	9.1	17.4	11.6	5.4	12.5	13.6	19.3	23.4	10.3	14.4	7.8	2.7
s_sound_skookum.cr	10.9	19.2	13.3	7.2	14.2	15.3	21.0	25.1	12.0	16.1	9.5	4.4
s_sound_coulter.cr	2.1	10.3	4.5	1.7	5.4	6.5	12.2	16.3	3.2	7.3	0.7	4.4
s_sound_burley.cr	6.1	14.4	8.5	2.4	9.4	10.5	16.2	20.3	7.2	11.3	4.7	0.4
s_sound_blackjack.cr	21.7	30.0	24.2	18.0	25.1	26.1	31.8	36.0	22.9	27.0	20.4	15.3
s_sound_gorst.cr	0.6	8.9	3.1	3.1	4.0	5.0	10.7	14.9	1.7	5.8	0.8	5.9
s_sound_clear.cr	1.0	7.3	1.5	4.7	2.4	3.5	9.2	13.3	0.2	4.3	2.3	7.4
s_sound_dogfish.cr	4.7	12.9	7.1	0.9	8.0	9.1	14.8	18.9	5.8	9.9	3.3	1.8
HOOD CANAL												
skokomish	0.0	17.8	8.9	14.7	1.5							
sf.skokomish.r	17.8	0.0	9.0	3.1	19.3							
hamma.hamma.r	8.9	9.0	0.0	5.8	10.4							
duckabush.r	14.7	3.1	5.8	0.0	16.2							
dosewallips.r	1.5	19.3	10.4	16.2	0.0							
STRAITS												
dungeness	0.0	21.1	4.1									
dungen_grey.wolf.r	21.1	0.0	25.2									
elwha.r	4.1	25.2	0.0									

Table B.7. Dissimilarity matrix (1-percent overlap) for smolt-spawner age distributions.

NOOKSACK	sf.nook	nf.nook						
sf.nook	0.00	0.32						
nf.nook		0.00						
SKAGIT	skagit	sauk	suiattle.buck	suiattle.lime	attle.sulphur	skag.illabot	cascade	scade.clark
skagit		0.32	0.38	0.48	0.69	0.45	0.40	0.64
sauk	0.32		0.19	0.27	0.46	0.42	0.27	0.59
suiattle.buck	0.38	0.19		0.12	0.31	0.36	0.18	0.53
suiattle.lime	0.48	0.27	0.12		0.27	0.37	0.28	0.54
suiattle.sulphur	0.69	0.46	0.31	0.27		0.48	0.37	0.48
up.skag.illabot	0.45	0.42	0.36	0.37	0.48		0.19	0.26
cascade	0.40	0.27	0.18	0.28	0.37	0.19		0.38
cascade.clark	0.64	0.59	0.53	0.54	0.48	0.26	0.38	
STILLAGUAMISH	nf.stilla	sf.stilla						
nf.stilla	0.00	0.11						
sf.stilla		0.00						
SNOHOMISH	snoqualmie	snoq.tokul	wallace	wallace.may				
snoqualmie	0.00	0.33	0.54	0.54				
snoq.tokul		0.00	0.62	0.64				
wallace			0.00	0.14				
wallace.may				0.00				
LK. WASHINGTON	cedar	nlk.wash	sammam	issaquah				
cedar	0.00							
nlk.wash		0.00						
sammam			0.00					
issaquah				0.00				
SOUTH SOUND	duwam.gr	green.bigsoo	green.newauk	puyal.voight	puyal.sprairi	deschutes		
duwam.gr	0.00	0.14	0.16	0.18	0.28	0.17		
green.bigsoos		0.00	0.25	0.09	0.14	0.13		
green.newaukum			0.00	0.32	0.31	0.28		
puyal.voight				0.00	0.18	0.11		
puyal.sprairie					0.00	0.22		
deschutes						0.00		
HOOD CANAL	skokomish	skok.purdy	hoodc.finch					
skokomish	0.00	0.09	0.13					
skok.purdy		0.00	0.19					
hoodc.finch			0.00					
STRAITS	dungen	elwha						
dungen	0.00	0.41						
elwha		0.00						

Table B.8. Absolute differences in mean spawner length (post-orbital hypural length of age-4 fish, cm) of Puget Sound chinook. Sexes and broodyears for each stock are pooled. Bold entries indicate significant heterogeneity in pairwise G-tests, using a basinwise Bonferroni-adjusted alpha-level (data source: WDFW).

NOOKSACK	sf.nook	nf.nook
sf.nook		**
nf.nook		**

SKAGIT	lw.skag	up.skag	lw.sauk	up.sauk	suiattle	cascade
lw.skag		**	4.58		4.61	
up.skag			**		9.19	
lw.sauk				**		
up.sauk					**	
suiattle						**
cascade						**

STILLAGUAMISH	nf.stilla	sf.stilla
nf.stilla		**
sf.stilla		4.75

SNOHOMISH	lw.snoh	skykom*	sultan	wallace	bridalveil	snoqual*
lw.snoh		**				
skykom			**	-1.53	8.85	6.79
sultan				**	10.37	8.32
wallace					**	
bridalveil						**
snoqual						-2.05

LK. WASHINGTON	cedar	nlk.wash	sammam	issaquah
cedar		**		
nlk.wash			**	
sammam				**
issaquah				

SOUTH SOUND	green.newaukum	puyal.sprairie	white	nisqually	deschutes	misc13a
green.newaukum		**	0.91	6.01		
puyal.sprairie			**	6.92		
white				**		
nisqually					**	
deschutes						**
misc13a						

Table B.9. Correlation coefficients on residuals from autoregressive trend model: product-moment correlations below diagonal, Spearman's rank correlations above. Bold entries indicate significant correlations using a basinwise Bonferroni-adjusted alpha level.

NOOKSACK	sf.nook	nf.nook						
sf.nook	1.00							
nf.nook		1.00						
SKAGIT	lw.skag	up.skag	lw.sauk	up.sauk	suiattle	cascade		
lw.skag	1.00	0.26	0.75	0.27	0.11			
up.skag	0.37	1.00	0.35	0.22	0.34			
lw.sauk	0.75	0.41	1.00	0.30	0.21			
up.sauk	0.07	0.20	0.16	1.00	0.12			
suiattle	0.21	0.38	0.28	0.07	1.00			
cascade						1.00		
STILLAGUAMISH	nf.stilla	sf.stilla						
nf.stilla	1.00	0.35						
sf.stilla	0.51	1.00						
SNOHOMISH	lw.snoh*	skykom	sultan	wallace	bridalveil	snoqual*		
lw.snoh	1.00			0.46		0.07		
skykom		1.00						
sultan			1.00					
wallace	0.43			1.00		0.08		
bridalveil					1.00			
snoqual	0.08			0.11		1.00		
LK. WASHINGTON	cedar	nlk.wash	sammam	issaquah				
cedar	1.00	0.19						
nlk.wash	0.62	1.00						
sammam			1.00					
issaquah				1.00				
SOUTH SOUND	duwam.gr	puyallup	white	nisqually	deschut	misc13	misc13a	misc13b
duwam.gr	1.00	0.21	-0.02	0.29	-0.10	0.02	-0.19	0.22
puyallup	0.25	1.00	0.08	0.41	0.65	0.18	-0.08	-0.22
white	0.01	0.13	1.00	-0.09	0.07	0.46	-0.10	0.08
nisqually	0.17	0.27	-0.01	1.00	-0.10	0.31	-0.20	0.06
deschut	-0.11	0.73	0.09	-0.10	1.00	-0.03	-0.39	0.06
misc13	0.02	0.25	0.59	0.41	0.02	1.00	0.00	-0.03
misc13a	-0.20	0.02	-0.06	-0.11	-0.35	0.13	1.00	-0.20
misc13b	0.06	-0.14	0.04	0.06	0.15	-0.03	-0.13	1.00
HOOD CANAL	skokom	hamma	ducka	dosewal				
skokom	1.00	0.18	0.09	-0.13				
hamma	-0.03	1.00	-0.33	0.67				
ducka	0.03	-0.44	1.00	-0.02				
dosewal	-0.09	0.76	-0.15	1.00				
STRAITS	dungen	elwha						
dungen	1.00	-0.04						
elwha	-0.18	1.00						

Table B.11. Absolute difference in mean temperature (C) during incubation for chinook in Puget Sound. Temperature was measured at USGS stations (corresponding to the rows and columns of the table) over variable time intervals. Annual incubation temperature is estimated as the mean temperature during the 3-month period beginning on the median date of spawning in the nearest chinook index survey area. Differences presented in the table are based on means over all years of available data. Bold entries indicate significant differences in two-sample t-tests using a basinwise Bonferroni-adjusted alpha level. Italics indicate that no test could be performed because fewer than 3 annual means were available.

[illegible]